Fracture 1977, Volume 2, ICF4, Waterloo, Canada, June 19 - 24, 1977

INFLUENCE OF GRAIN SIZE ON THE FRACTURE OF ALUMINUM ALLOYS

G. Lütjering*, T. Hamajima* and A. Gysler**

INTRODUCTION

It has been proven for many alloys especially for the lower yield point of steels, that the grain size has an influence on the tensile yield stress. However, an influence of grain size on other mechanical properties such as ductility, fatigue properties, and crack propagation is still uncertain. Recently it was shown for a variety of Ti-alloys [1, 2] and for an austenitic steel [3] that the tensile ductility increased with decreasing grain size. For some microstructures an effect of grain size on crack propagation was reported [3, 4] but the results are still contradictory [5]. For Al-alloys it was shown that the true fracture stress increased with decreasing grain size [6].

The purpose of the present work was to investigate the influence of grain size on the fracture behaviour of high strength Al-alloys for two different deformation and fracture mechanisms [7] which are shown schematically in Figure 1. Mechanism A is observed for alloys containing particles which can be sheared by the moving dislocations leading to the formation of intense slip bands. These slip bands are able to produce offsets in grain boundaries (crack nucleation sites) and a transcrystalline fracture occurs along these intense slip bands. If upon aging precipitate-free zones (PFZ) develop along grain boundaries preferred plastic deformation occurs within these weak zones and cracks are nucleated presumably at grain boundary triple points. The fracture is then intercrystalline (mechanism B).

EXPERIMENTAL PROCEDURE

The investigation was performed on a high purity Al-5.7 wt.-% Zn-2.5% Mg-1.5% Cu alloy, supplied by the Schweizerische Aluminium AG, Neuhausen, Switzerland. Due to the high purity almost no inclusions were present in this alloy. Homogenization of the alloy at 738K for 1 hour followed by quenching in ice-water produced a grain size of 220 μm. A small grain size of 30 μm was obtained by the following additional steps: Aging at 653K for 5 hours to precipitate coarse η-particles, immediately after ice-water quenching from 653K cold rolling to a deformation degree of $\phi = 0.69$, recrystallization at 653K and homogenization at 713K both for 10 minutes and both followed by ice-water quenching. All specimens were kept at room temperature for about 2 days before aging them at 373K and 433K for various times.

Tensile tests were carried out on round specimens with a diameter of 6 mm and a gage length of 25 mm. The strain rate was $6.7 \times 10^{-4}\ s^{-1}$.

* Ruhr-University, Bochum, Germany.
**DFVLR, Cologne, Germany.

The fracture surface was investigated by scanning electron microscopy. Fatigue life tests were performed on round electrolytically polished specimens (diameter 4 mm) under push-pull loading at constant stress amplitudes with a frequency of 110 Hz. The nucleation of fatigue cracks was studied by light microscopy.

RESULTS

The dependence of tensile properties on aging time at 373K is shown in Figure 2 for specimens with the large grain size of 220 μm. The yield stress $\sigma_{0.2}$ increased continuously whereas the true fracture strain ε_F declined.

The true fracture stress σ_F reached a slight maximum after 100 h aging time. The observed fracture mechanisms are indicated above the curves in Figure 2. In the as-quenched condition and after short aging times the fracture mechanism is a dimple type rupture through the matrix (region marked "DIMPLE" in Figure 2). The dimples stemming from the few inclusions present in the alloy. With increasing aging time intense slip bands are formed upon plastic deformation leading to a transcrystalline fracture along slip bands (mechanism A in Figure 1). This fracture mechanism is observed in the region marked "SLIP BANDS" in Figure 2. After an aging time of 1000 h at 373K narrow precipitate-free zones are formed along grain boundaries which deform preferentially and fracture mechanism B (Figure 1) is observed indicated by "GB (PFZ)" in Figure 2.

The dependence of tensile properties on aging time at 433K is shown in Figure 3 again for specimens with the large grain size of 220 μm. At this higher aging temperature the yield stress passes through a maximum indicating that the alloy can be overaged at 433K. The ductility ε_F goes through a pronounced minimum reaching the low value of 0.08. The fracture stress exhibits again a slight maximum in this case at short aging times. Also shown in this figure are the results obtained on specimens aged at 180°C for 48 hours to include a completely overaged structure. As expected the yield stress decreased whereas the ductility increased. The observed fracture mechanisms which are indicated again above the curves in Figure 3 showed the same tendency in variation with increasing aging time as at 373K (Figure 2). At 433K aging temperature the region in which fracture mechanism A occurred was confined to short aging times. The dominant fracture mechanism was now the intercrystalline fracture mode B induced by preferential plastic deformation within PFZ. Plastic deformation of the matrix still occurred within slip bands. It should be mentioned that upon further overaging again a dimple type of transcrystalline rupture appeared, the dimples stemming then from particles of the equilibrium η-phase.

For the investigation of the influence of grain size on mechanical properties for the two deformation and fracture mechanisms A and B two characteristic aging treatments were chosen: 24 h at 373K for mechanism A and and 20 h at 433K for mechanism B.

Fracture Mechanism A

The tensile properties for the two grain sizes investigated are shown in Table 1. It can be seen that the yield stress $\sigma_{0.2}$ did not vary within experimental error. With decreasing grain size the true fracture stress σ_F increased and also the true fracture strain ε_F from 0.35 to 0.65. The

corresponding fracture surfaces are shown in Figure 4. For the large grain size of 220 μm the typical step-like transcrystalline fracture along slip bands dominates the whole fracture surface (Figure 4a). For the small grain size of 30 μm this type of fracture mode was observed only occasionally (Figure 4b). Most portions of the fracture surface were covered with dimples having an average spacing of 1 - 2 μm. These distances are comparable to the observed slip band spacings. The results of the fatigue life tests for the two grain sizes are plotted in Figure 5 in form of S-N curves. It can be seen that the fatigue life was longer for specimens with the small grain size over the whole range of stress amplitudes investigated. The light microscopic study of the specimen surfaces proved that cracks nucleated much earlier in specimens with the large grain size amounting to premature failure. For both grain sizes cracks nucleated at intense slip bands (Figure 6). The slip bands were much more pronounced in specimens with the large grain size (Figure 6a) as compared to specimens with an average grain size of 30 μm (Figure 6b). For these latter specimens cracks at slip bands could only be detected in grains which were statistically larger than average (see centre part of Figure 6b). It was not possible to prove whether the cracks nucleated within slip bands or by the interaction of slip bands with grain boundaries.

Fracture Mechanism B

A comparison of the tensile properties for the two grain sizes is given in Table 2. Again no difference in yield stress $\sigma_{0.2}$ was found. Both the true fracture stress σ_F and the true fracture strain ε_F increased with decreasing grain size for this deformation and fracture mechanism B. The increase of ε_F from 0.10 to 0.42 is remarkable. The corresponding fracture surfaces revealed that for the large grain size the typical ductile fracture along grain boundaries covered the whole surface (Figure 7a) whereas for the small grain size the portions showing a dimple type of transcrystalline fracture mode increased (Figure 7b). The dimple spacings were similar to those observed for specimens aged 24 h at 373K (see Figure 4b). On the flat grain surfaces small dimples become visible at higher magnifications resulting from interfacial decohesion of the incoherent η-particles present at the grain boundaries.

The influence of grain size on the fatigue life was investigated and the results can be seen in Figure 8. The specimens with the small grain size of 30 μm exhibited longer fatigue lives as compared to specimens with 200 μm grain size. Light microscopic investigation of the specimen surfaces showed that this difference was due to a difference in crack nucleation period. In Figure 9 specimens are compared which were fatigued with a stress amplitude of 200 MPa. Specimens with the large grain size showed pronounced preferential deformation along grain boundaries inclined about 45° to the loading direction (indicated by arrows in Figure 9). Cracks appeared along grain boundaries oriented mainly perpendicular to the loading axis. For the large grain size cracks also were nucleated at grain boundaries parallel to the loading axis (Figure 9a) but these cracks did not grow further. For specimens with the small grain size it was difficult to detect cracks (small arrows in Figure 9b) but then they were always aligned perpendicular to the loading direction.

Fracture toughness tests as well as fatigue crack propagation measurements in vacuum were performed for the two grain sizes in condition A (24 h 373K and B (20 h 433K). Based on these preliminary results it can be said that at least no improvement of crack propagation properties was found with decreasing grain size.

DISCUSSION

For the high strength aluminum alloy investigated the results of tensile tests are in agreement with the view that an inhomogeneous distribution of plastic deformation induced by weak zones (sheared particles for mechanism A and PFZ for mechanism B) has a deleterious effect on the macroscopic mechanical properties [7]. This deleterious effect increases with increasing difference in flow stress between weak and hardened zone explaining the observed dependence of tensile ductility on aging time (Figures 2 and 3). A pronounced effect of grain size was found on crack nucleation for the two different deformation and fracture mechanisms A and B (Figure 1). In both cases a reduction in slip length [1, 2] (grain diameter for mechanism A and grain boundary length for mechanism B) leads to reduced stress concentrations delaying crack nucleation and improving therefore the tensile fracture properties (Tables 1 and 2) and the fatigue properties (Figures 5 and 8). For tensile experiments this delay in crack nucleation for mechanisms A and B leads to the appearance of a different crack nucleation mechanism for specimens with the small grain size of 30 µm. Voids are nucleated within the matrix at intersecting slip bands [8] which coalesce and form dimples visible on the fracture surfaces (Figures 4b and 7b).

The difference in crack nucleation mechanism for the deformation modes A and B can be clearly seen by comparing the appearance of fatigue surface cracks (Figures 6 and 9). For the case of preferred plastic deformation within PFZ (mode B) cracks appeared perpendicular and parallel (push-pull loading) to the loading direction (Figure 9a). This proves that the cracks nucleated at grain boundary triple points induced by pronounced plastic deformation within PFZ along boundaries lying at an angle of about 45° to the loading direction [2].

Although a pronounced influence of grain size on crack nucleation was found there seems to be no or only a small effect on crack growth. The fact that no difference in yield stress $\sigma_{0.2}$ between specimens with grain sizes of 220 µm and 30 µm was found in this work as well as for some Ti-alloys [1, 2] raises the question which microstructural conditions are responsible for the dependence of yield stress on grain size observed for many other alloys.

ACKNOWLEDGEMENT

This work was supported by the Deutsche Forschungsgemeinschaft.

REFERENCES

1. GYSLER, A., TERLINDE, G. and LÜTJERING, G., Proc. 3rd Int. Conf. on Titanium, Moscow, 1976.
2. PETERS, M. and LÜTJERING, G., Z. Metallkunde, 67, 1976, 811.
3. ZUM-GAHR, K. H. and EBERHARTINGER, L. J., Z. Metallkunde, 67, 1976, 640.
4. HORNBOGEN, E., Proc. Fourth Int. Conf. on Strength of Metals and Alloys, Nancy, France, 1976, 555.
5. THOMPSON, A. W. and BUCCI, R. J., Met. Trans., 4, 1973, 1173.
6. EVENSEN, J. D., RYUM, N. and EMBURY, J. D., Mat. Sci. Eng., 18, 1975, 221.
7. LÜTJERING, G., ESA TT-245, 1976.

8. GYSLER, A., LÜTJERING, G. and GEROLD, V., Acta Met., 22, 1974, 901.

Table 1 A: 24 h 373K
Tensile properties for two grain sizes

GRAIN SIZE	$\sigma_{0,2}$ [MPa]	σ_F [MPa]	ε_F
220 µm	420	720	0.35
30 µm	420	840	0.65

Table 2 B: 20 h 433K
Tensile properties for two grain sizes

GRAIN SIZE	$\sigma_{0,2}$ [MPa]	σ_F [MPa]	ε_F
220 µm	480	570	0.10
30 µm	480	690	0.42

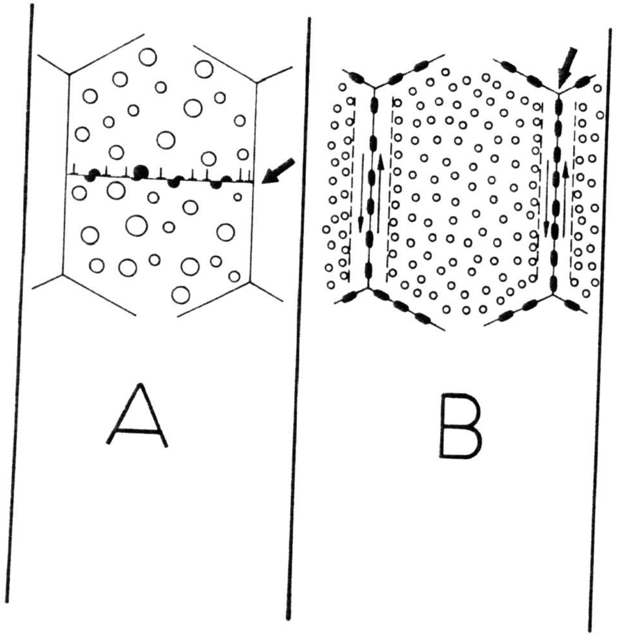

Figure 1 Deformation and fracture mechanisms investigated (schematically).
A: Slip band fracture B: Grain boundary fracture (PFZ)

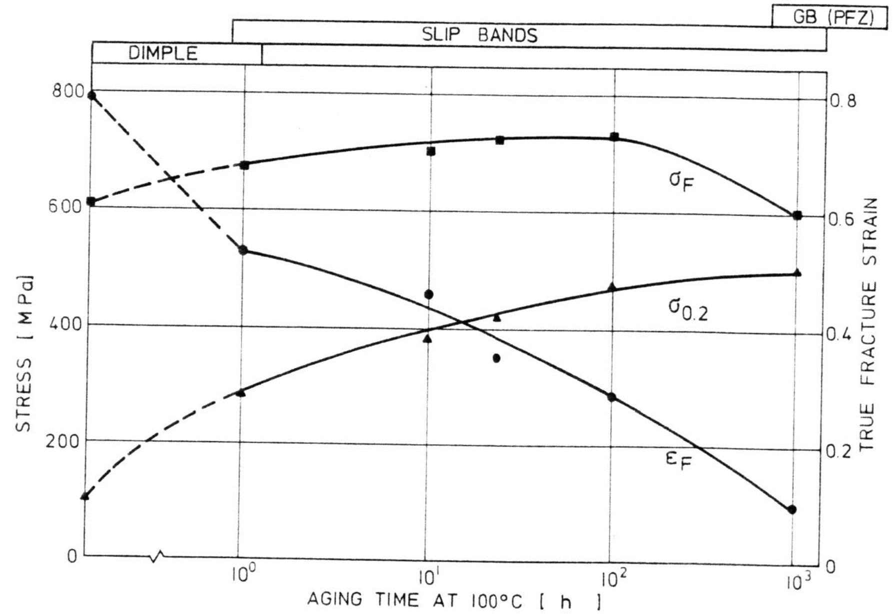

Figure 2 Tensile properties ($\sigma_{0.2}$, σ_F, ε_F) versus aging time at 373K

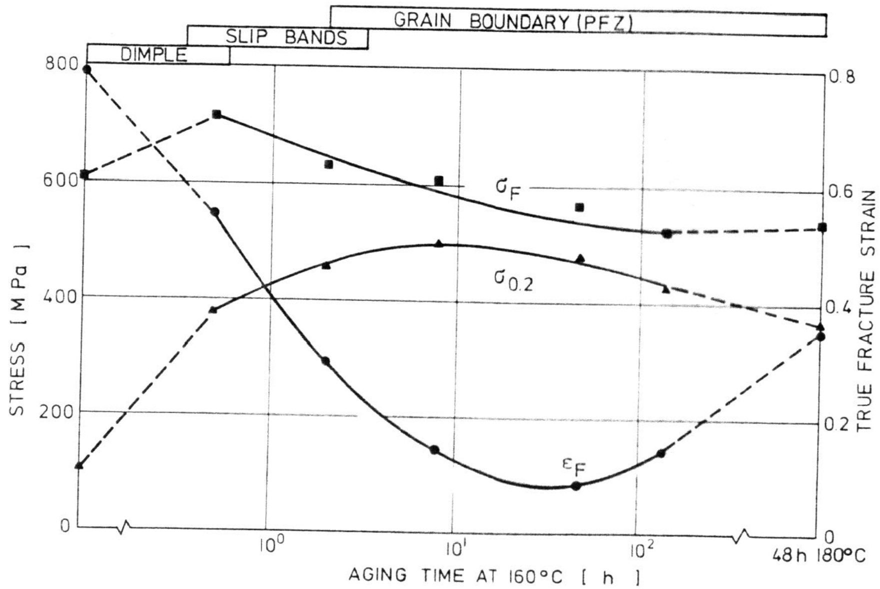

Figure 3 Tensile properties ($\sigma_{0.2}$, σ_F, ε_F) versus aging time at 433K.

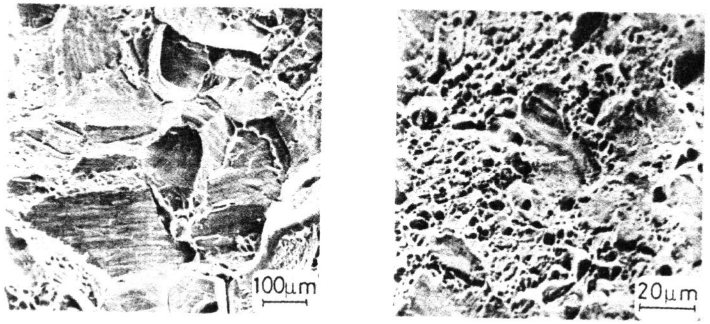

(a) (b)

Figure 4 A: 24 h 100° C

Tensile Fracture Surface (SEM)

(a) Grain size 220 µm, ε_F = 0.35.
(b) Grain size 30 µm, ε_F = 0.65.

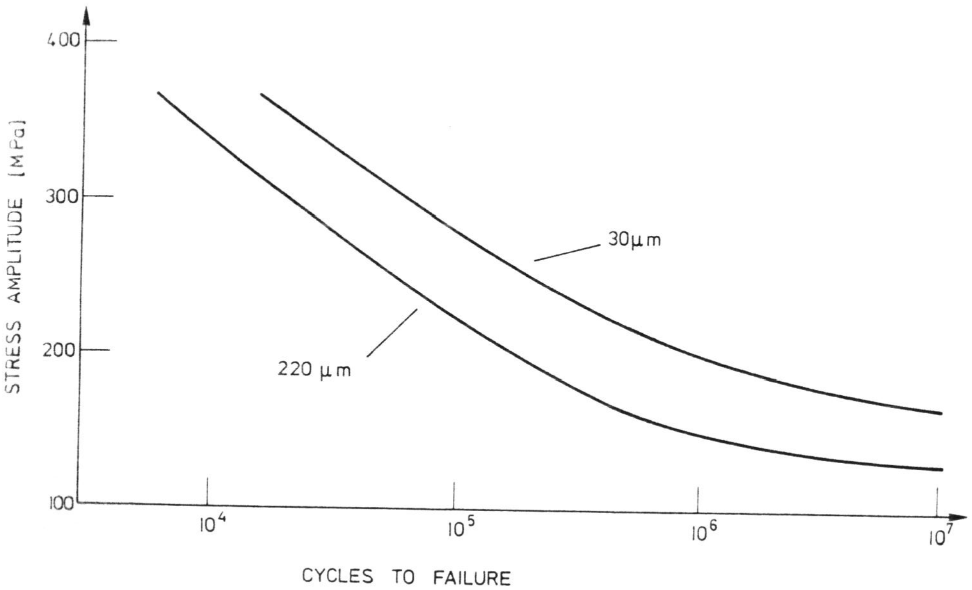

Figure 5 A: 24 h 373K

S-N curves for two grain sizes (220 µm and 30 µm)

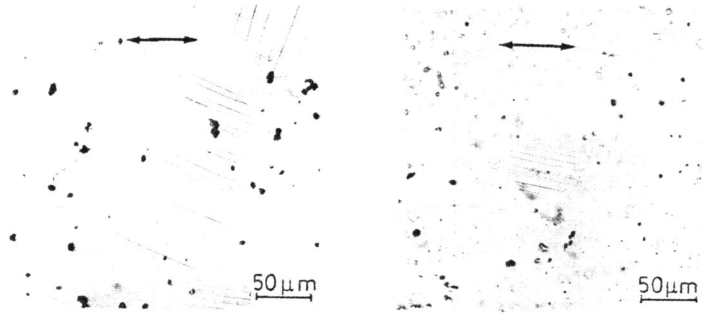

(a) (b)

Figure 6 A: 24 h 373K

Fatigue crack nucleation, $\sigma = \pm$ 200 MPa, (LM)

(a) Grain Size 220 µm, N_F = 300 000 cycles

(b) Grain size 30 µm, N_F = 1 350 000 cycles

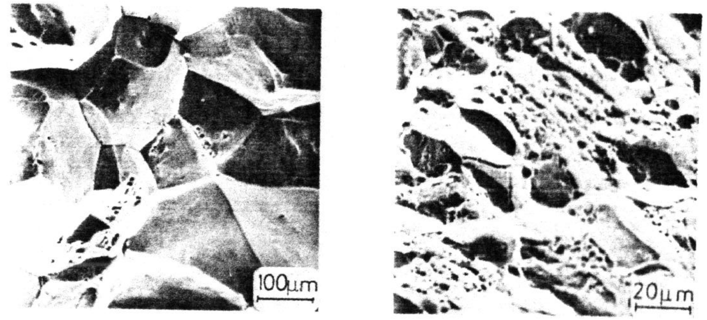

(a) (b)

Figure 7 B: 20 h 433K

Tensile fracture surface (SEM)

(a) Grain size 220 µm, ε_F = 0.10

(b) Grain size 30 µm, ε_F = 0.42

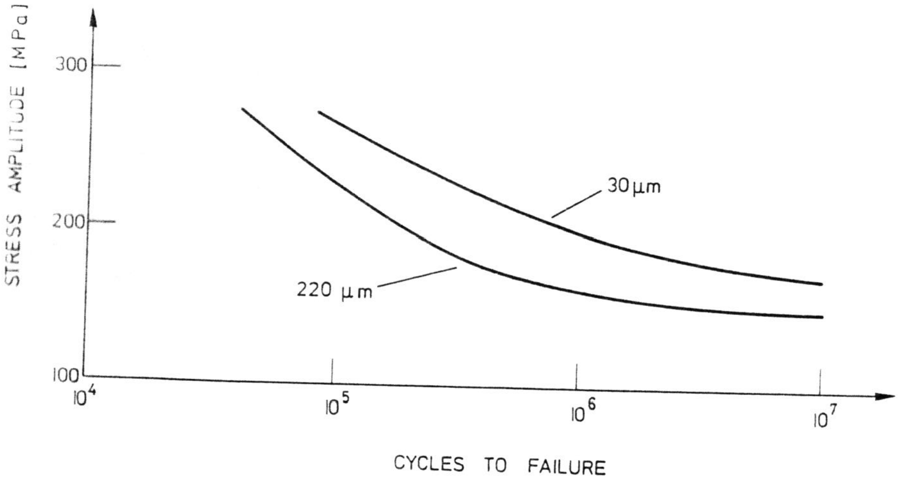

Figure 8 B: 20 h 433K
S-N curves for two grain sizes (220 µm and 30 µm)

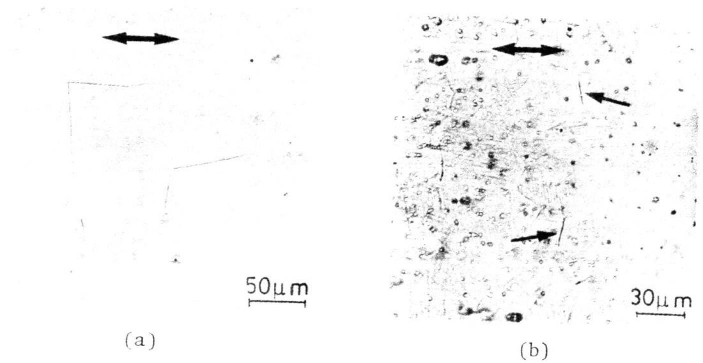

Figure 9 B: 20 h 433K
Fatigue crack nucleation, $\sigma = \pm\ 200$ MPa, (LM)
(a) Grain size 220 µm, N_F = 200 000 cycles
(b) Grain size 30 µm, N_F = 700 000 cycles